Six-Axis Vibrational Power Transducer for Active Vibration Isolation

Carl Q. Howard (1) and Colin H. Hansen (1)

(1) School of Mechanical Engineering, The University of Adelade, Adelaide, S.A. 5005, Australia

ABSTRACT

A transducer is described which can be used to measure the translational and rotational vibratory power transmission from a source to a receiving structure. A description of the procedure used to calibrate the device is also included. The results from the calibration show that whilst the amplitude of the forces, moments, translational and rotational displacements can be measured accurately, it is the phase accuracy of these measurements that limit the accuracy of measurements of vibratory power transmission. The transducer was used in active vibration isolation experiments to reduce the vibration energy transmitted into a beam from a vibrating rigid mass. The results show the occurrence of vibratory power circulation where translational vibration is converted into rotational vibration.

INTRODUCTION

The transmission of vibration from one structure to another always involves the transmission of both vibratory forces and vibratory moments along translational and rotational axes respectively. However, there are few measurement transducers capable of measuring both forces and moments simultaneously. Researchers frequently ignore the contribution of rotational power transmission when attempting to determine the total vibrational power transmitted from one structure to another, which usually leads to an underestimate of the vibratory power transmission. However, previous work has shown that the vibrational power transmission from rotational moments cannot be neglected (Petersson and Gibbs, 1990; Petersson, 1993a,b; Koh and White, 1997a,b,c; Howard and Hansen, 1999; Sanderson et al., 1995; Mondot and Moorhouse, 1996; Sanderson, 1996; Gialamas et al., 1996; Gibbs and Yap, 1998; Moorhouse, 2002; Shepard Jr., 2002; Ji et al., 2003; Yap and Gibbs, 1999a,b; Bardou et al., 1997).

This paper reports work on the development and testing of a transducer which is capable of measuring motion, forces and moments for all six degrees of motion. The transducer is used in an active vibration isolation experiment to measure power transmission along translational and rotational axes. The transducers consists of an array of strain gauges mounted to an aluminium mandrel to measure forces and moments, and an array of accelerometers to measure the translational and rotational motion of the force transducer. Practical difficulties associated with the use of power transmission as a cost function and the power circulation or negative power transmission phenomenon are demonstrated.

CALCULATION OF POWER TRANSMISSION

The time averaged vibratory power transmission for tonal vibrational defined as half the real part of the force f multiplied by the complex conjugate of the velocity v and is given by (Skudrzyk, 1968) as:

$$\langle fv \rangle_t = \frac{1}{2}\mathrm{Re}(fv^*) = FV\cos(\theta) \qquad (1)$$

where F and V are the amplitudes of the force and velocity response, and θ is the phase angle between the force and velocity signals. For the case where the velocity at a point on a structure to be 90 degrees out of phase with the driving force, then using Eq. (1) the power transmitted into the structure is zero. If the instruments measuring the force and velocity result in a 1 degree error in phase, then the percentage error of the measured power to the actual power is infinite! Clearly, this equation shows that as well as the importance of accurate amplitude measurements of force and velocity, the accurate measurement of the relative phase angle is also important in the determination of vibratory power transmission, especially in situations where the reactive vibrational field is large compared to the transmitted field.

In addition to the measurement of force, the measurement of vibratory power transmission requires the accurate measurement of the velocity of the structure at the point where the force is measured. A discussion of the measurement of force is included in the next section and a discussion of the measurement of velocity is included in the section after that.

TRANSDUCERS TO MEASURE OF FORCES AND MOMENTS

Since the beginning of the 1980's several types of 6-axis force transducer have been commercially available for use on the end of robot arms used in manufacturing industries. Two companies which sell such products are ATI Industrial Automation and JR3, both from the United States. Unfortunately both systems were not suitable for active control experiments because neither system has suitable analog outputs which can be used to calculate power.

Another company called Robert A Denton, from the United Kingdom, assembles off-the-shelf force transducers into a package to measure forces along 6 axes. These force transducers are used in automobile crash testing where the loads are impulsive and extremely high and therefore unsuitable for active control experiments where the loads are continuous and small compared to impact testing.

Engeler and Giorgetta (1995) describe a 6-axis force transducer which uses specially shaped piezo-electric crystals which was intended for use inside a joystick. The adaptation of this design to measure forces between a vibration isolator

and receiving structure would be too difficult, as special purpose piezo-electric crystals would be needed.

Kaneko (1996) gives a good overview of the development of 6-axis force transducers and describes some commercially available products. He used two 3-axis force transducers to make a 6-axis force transducer. The 3-axis force transducers were packaged as an integrated circuit. This product sounded extremely attractive, but after contacting the manufactures of the integrated circuit (and their competitors), this type of product was found not to be commercially available. No reasons were given by the companies.

Quinn and Mote Jr. (1990) describe a 6-axis force transducer to measure the force that a cyclist applies to pedals while cycling. The ingenious design uses strain gauges mounted to shear panel elements. The shear panel elements were used to reduce the cross-axis sensitivity of the sensor. A design using this method was examined by the author but it was found that large displacements of the shear panels would occur which would cause resonance problems.

Due to the lack of suitable commercial 6-axis force transducers, and the high cost of commercially available 3-axis force transducers, it was decided to develop a custom built 6-axis force transducer for the experimental work presented here.

DESCRIPTION OF THE MULTI-AXIS FORCE AND MOMENT TRANSDUCER

A 6-axis force transducer was developed and a schematic of the device is shown in Figure 1. This force transducer uses 24 strain gauges mounted to a cylindrical tube to measure forces and moments along all six axes (*Fx*, *Fy* , *Fz* , *Mx*, *My* and *Mz*). Figure 2 shows a close up view of the strain gauges mounted to the cylindrical tube. The outer dimensions of the sensor are 70mm outside diameter and 50mm high.

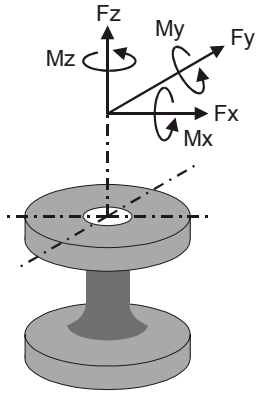

Figure 1: Schematic of 6-axis force transducer.

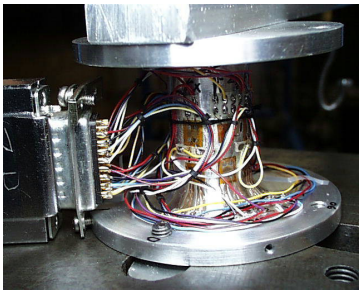

Figure 2: Close-up photo of the 6-axis force transducer.

For the 6-axis force transducer shown above, a group of four strain gauges are combined to form a full bridge Wheatstone circuit, which measures the force or moment along a single axis. The full bridge circuit has advantages in increased sensitivity (4 times greater compared to a quarter bridge), negligible thermal effects and decreased cross-axis sensitivity. Each group of four strain gauges is orientated to reject off-axis loads (Hoffmann, 1976). Further details about the design of this transducer and the technique used to reduced the cross-axis sensitivity can be found in Howard (1999).

An advantage of using a force transducer made with strain gauges compared to piezoelectric crystals is that the transducer can be calibrated using static loads. Force transducers that use piezoelectric crystals can only be calibrated with dynamic loads. The disadvantage of using a force transducer utilising strain gauges is that the device must have some flexibility so that strain in the body can be measured, which has the potential for introducing unwanted resonances into the system under investigation.

MEASUREMENT OF VELOCITY

The question arises: where should the accelerometers be placed to measure the velocity of the structure beneath the strain gauges? To answer this question, a finite element model was constructed of one experimental setup used in this paper, as shown in figure 3. A vibrating rigid body was attached to a viscoelastic spring which isolated the vibration from a simply supported beam.

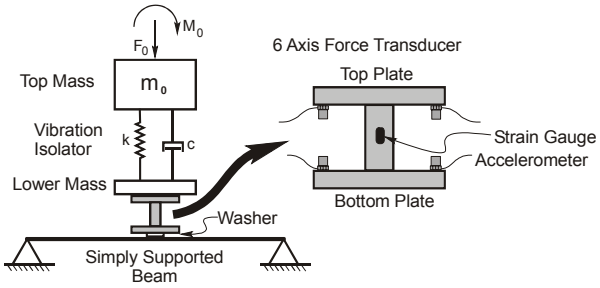

Figure 3: Schematic of the FEM to determine where to locate the accelerometers.

At the bottom of the vibration isolator is a lumped mass which is attached to the 6-axis force transducer. The force transducer sits on a 1mm thick washer and is attached to the simply supported beam. The washer is used to reduce the area of the transducer which is in contact with the beam, so that a more concentrated point load can be applied to the beam. The 6-axis force transducer is modelled as a cylindrical tube with a plate attached to each end of the tube. The cylindrical tube had an outside diameter of 22mm, an inside diameter of 20mm and a length of 40mm. The top and bottom plates have an outside diameter of 60mm and a thickness of 15mm. The simply supported beam was 25mm wide, 25mm thick and 1.495m long.

The axial velocity beneath the strain gauge can be accurately approximated by measuring the velocity at the top and bottom plates.

The measurement of the rotational velocities (θx and θy) at the location of the strain gauges on the force transducer is made difficult by the low bending stiffness of the cylindrical tube compared to the bending stiffness of the simply supported beam. A practical location to measure the rotational velocity would have been to mount accelerometers to the beam along the axial direction on both sides of the attachment point of the force transducer to the beam. Finite element modelling showed that this would provide a poor estimate of the actual rotational velocities. A better approximation of the rotational velocity at the strain gauge can be made by measuring the angular velocities of the top

and bottom plates and interpolating between the two measurements. The results obtained using this latter technique are shown in Figure 4. The angular velocity of each plate can be measured by using two accelerometers placed on opposite edges of plate, calculating the difference between the two translational velocities measured with the accelerometers and dividing by the distance which separates them.

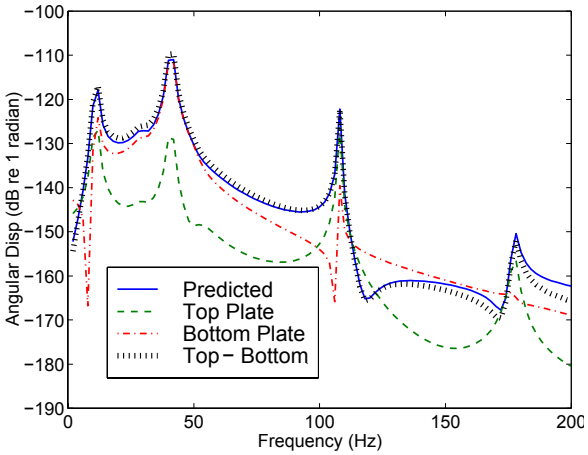

Figure 4: Predicted angular displacements of the top and bottom plates on the force transducer.

The results from the finite element analyses show that the angular velocity at the strain gauge can be reasonably approximated by the difference in the angular velocities of the top and bottom plates.

CALIBRATION

Static Calibration

Figure 5 shows how the 6-axis strain gauge force transducer was calibrated with static loads. The force transducer was mounted to an angle plate and secured to a table. A beam was bolted to the top flange of the transducer and a mass was hung from a hook on the end of the beam. Several masses and orientations of the transducer were used to determine the on-axis and cross-axis sensitivities of the sensor. The cross-axis sensitivity of each axis is approximately 20dB below the axial sensitivity. Typical piezoelectric type multi-component force transducers have cross-axis sensitivities of -40dB (1%) relative to the axial sensitivity..

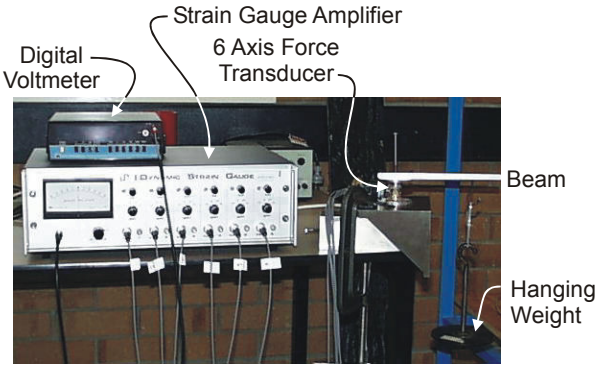

Figure 5: Static calibration of the force transducer.

Dynamic Calibration

An experiment based on Newton's second law, the acceleration of a mass is proportional to the applied force, was performed to measure the phase accuracy of this 6-axis force transducer. The experimental setup is shown in figure 6. For this test, the 6-axis force transducer was attached to a steel mass, which was hanging vertically. A Bruel and Kjær Type 8200 force transducer was attached to the 6-axis force transducer and a Bruel and Kjær Type 4393 accelerometer was attached to the back of the hanging mass. The Bruel and Kjær transducers were electrically connected to Bruel and Kjær Type 2635 charge amplifiers. The system was vibrated horizontally with band limited random excitation.

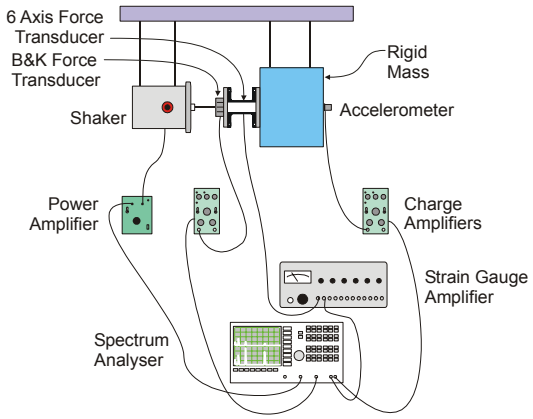

Figure 6: Dynamic calibration along the z-axis.

Figure 7 and Figure 8 shows the comparison of the amplitude and phase accuracy of the 6-axis force transducer compared with an accelerometer mounted to the rigid mass. The results show that there is a variation in amplitude of about ±0.1dB and a random variation in phase of about ±1 degrees, with a bias offset of about 1 degree. The bias phase error is caused by the filters in the analog strain gauge amplifiers which can be corrected by digital filtering (Horner and White, 1990). Although not shown, the coherence for these measurements was greater than 0.9. The experimental results presented here, which use the force signals from this transducer, have been corrected to take account of this bias phase error. The random phase errors cannot be corrected.

An experiment was undertaken to verify that the 6-axis force transducer could be used with an accelerometer array to measure power transmission into a simply supported steel beam. Figure 9 shows the experimental setup. The 6-axis force transducer was bolted at 0.75m along a simply supported beam of dimension 1.5m length, 25mm square and a steel washer was placed between the force transducer and the beam. The washer was used to reduce the area of the transducer which is in contact with the beam, so that a more concentrated point load could be applied to the beam. An aluminium bar was attached the top of the force transducer to simulate a cantilever. The axis of the aluminium bar was parallel with the axis of the beam. Five accelerometers were attached to the beam to measure an approximation of its kinetic energy. The accelerometers were located at 0.30m, 0.35m, 0.40m, 0.45m and 0.50m from the end of the beam. The frequency range of interest is between 0-200Hz, which corresponds to the first 3 vibration modes of the beam. A shaker was attached to the end of the cantilevered beam through a Bruel and Kjaer Type 8200 force transducer, which was used to measure the force applied by the shaker. Accelerometers were attached to the top and bottom plates on the force transducer as shown in Figure 3.

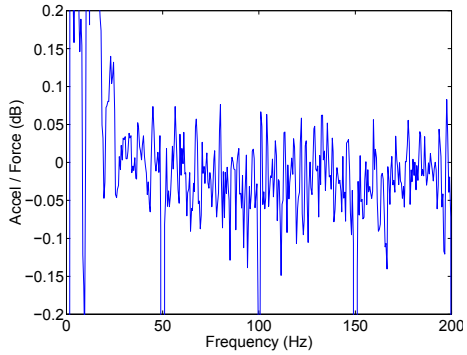

Figure 7: Amplitude accuracy of the force transducer along the z-axis.

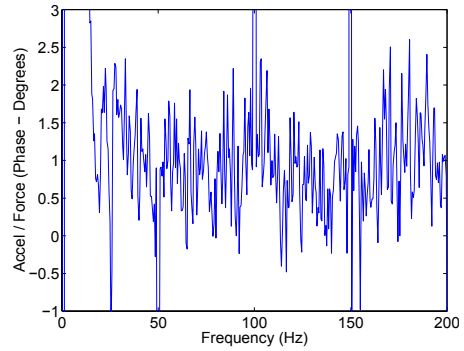

Figure 8: Phase accuracy of the force transducer along the z-axis.

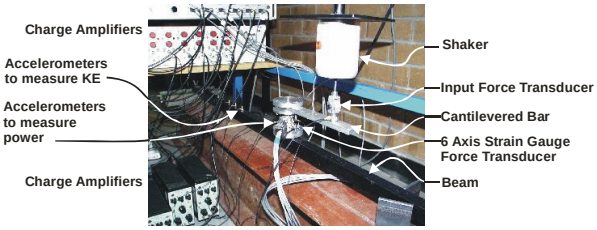

Figure 9: Experimental setup for the dynamic calibration of the multi-axis power transducer.

Using the software package Ansys, a Finite Element Model was constructed of the experimental setup described above. The model was constructed so that predictions could be made of the forces, displacements, power transmission from the shaker into the beam, and kinetic energy in the beam, which could be compared with the experimentally measured values. In addition, the results from this experiment are used to justify the method used to predict the velocity of the structure beneath the strain gauges, which is used in the calculation of the vibratory power transmission.

Figure 10 and Figure 11 show three curves for the vertical and angular displacements of the top and bottom plates: the predicted displacements using FEA of the structure beneath the strain gauges used to measure the axial force and bending moments are labelled 'Theory – Actual', the predicted displacements using FEA of the interpolated displacements on the edges of the plates which are remote from the location of the strain gauges are labelled 'Theory – Predicted', and the experimental measurements that use transducers that are remote from the strain gauges are labelled 'Experiment'. It can be seen that the results compare favourably. The divergence in the experimental results and predictions at low frequencies (>30Hz) is caused by a poor signal to noise ratio.

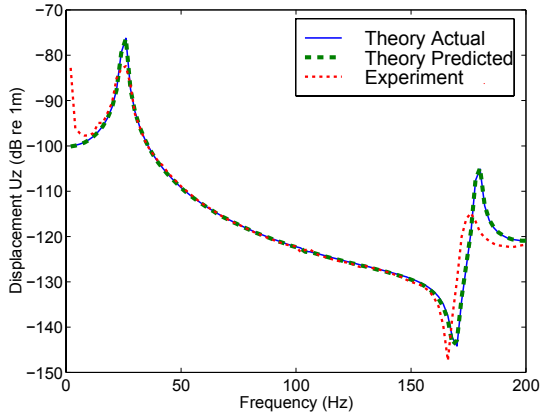

Figure 10: Comparison between theoretically predicted and experimentally measured displacement along the z-axis.

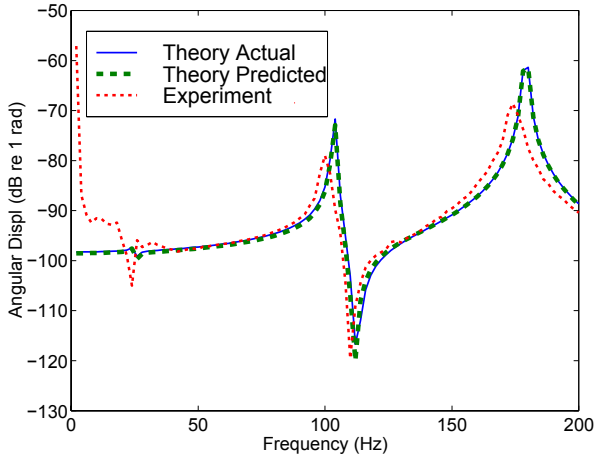

Figure 11: Comparison between theoretically predicted and experimentally measured angular displacement of the material beneath the strain gauges.

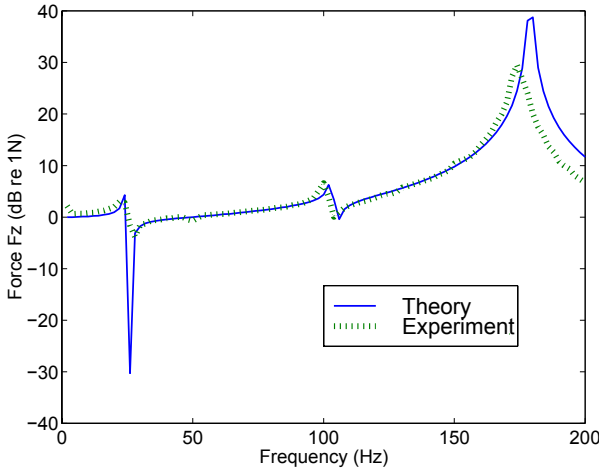

Figure 12: Comparison between theoretically predicted and experimentally measured force along the z-axis.

At high frequencies (>150Hz) the discrepancies are caused by inaccuracy in the finite element model not modelling the joint stiffness between the transducer and the beam.

The force along the vertical *z*-axis and the bending moment along the □y-axis are presented in Figure 12 and Figure 13 respectively. The experimental results compare favourably with the theoretical predictions.

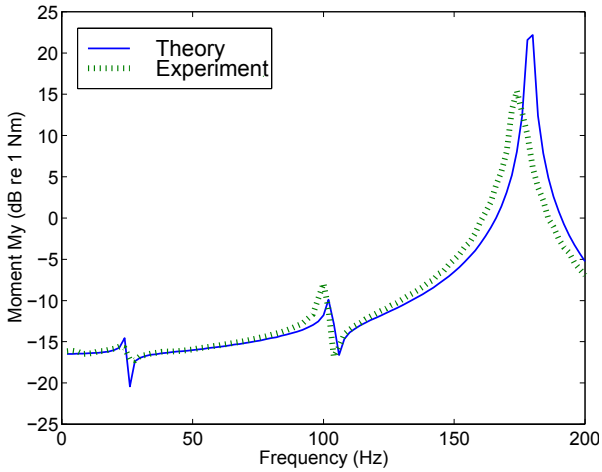

Figure 13: Comparison between theoretically predicted and experimentally measured bending moment along the θy-axis.

The calculation of power transmission into the simply supported beam requires a high degree of phase accuracy because the beam is very lightly damped. Figure 14 and Figure 15 show the predicted and measured power transmission into the beam along the vertical *z*-axis and around the θy-axis respectively.

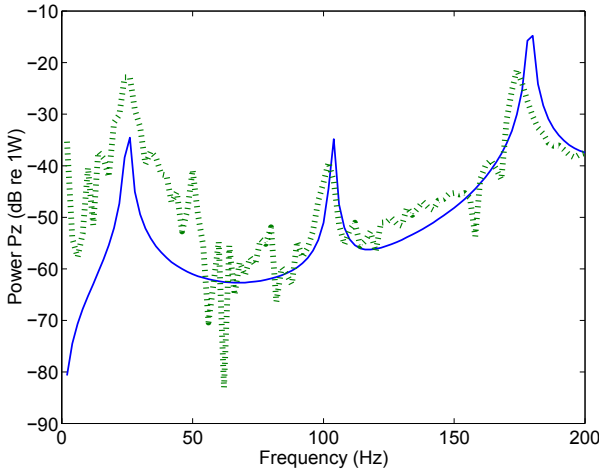

Figure 14: Comparison between theoretically predicted and experimentally measured power transmitted along the z-axis.

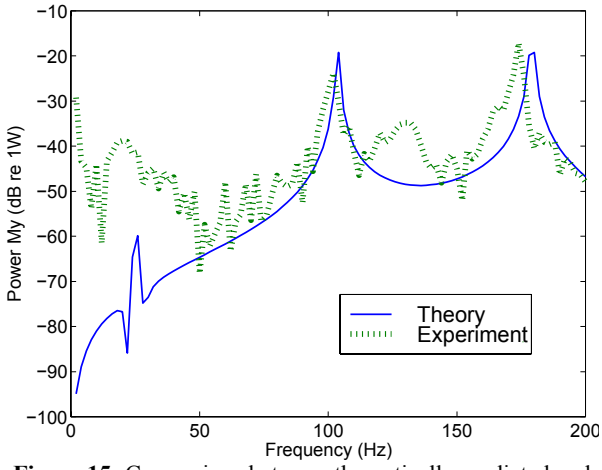

Figure 15: Comparison between theoretically predicted and experimentally measured power transmitted along the θy-axis.

The power transmission by rotational moments shown in Figure 15 indicate poor agreement between theory and experiment below 50Hz, which is due to the resonance of the shaker support. Figure 16 shows the phase angle of the rotational displacement of the structure beneath the strain gauges used to measure bending moments. It can be seen that between 0-50Hz, the phase angle passes through a 90 degree phase shift, which corresponds to a rotational resonance that is not taken into account by the theoretical model. The general scatter of experimental results around the theoretical predictions is due to the phase errors that were described earlier.

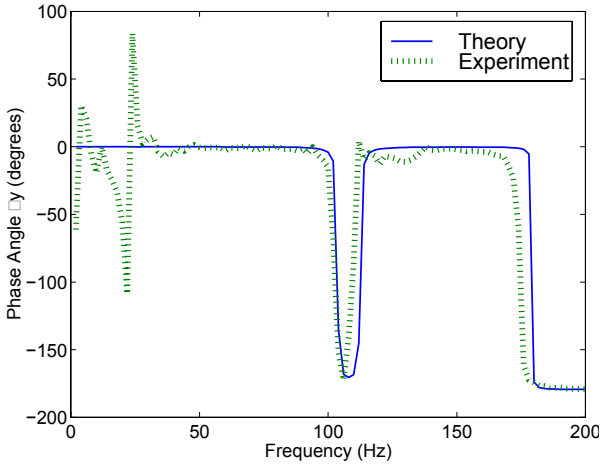

Figure 16: Comparison between theoretically predicted and experimentally measured phase angle for the rotational displacement along the θy-axis.

ACTIVE VIBRATION CONTROL EXPERIMENT

Experimental Setup

An active vibration isolation experiment was conducted that utilised the multi-axis power transducer described here. Figure 17 shows how the instruments were connected and Figure 18 shows a photo of the experimental rig.

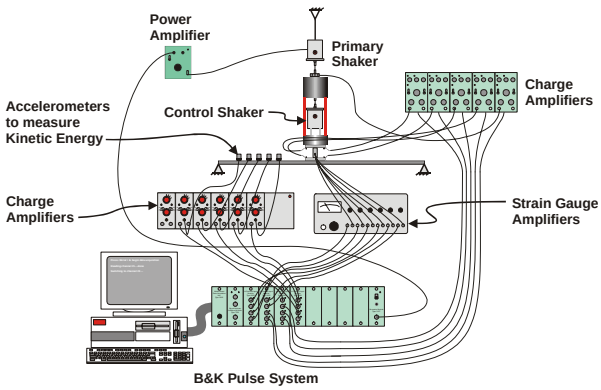

Figure 17: Instrumentation setup for the active vibration isolation experiment.

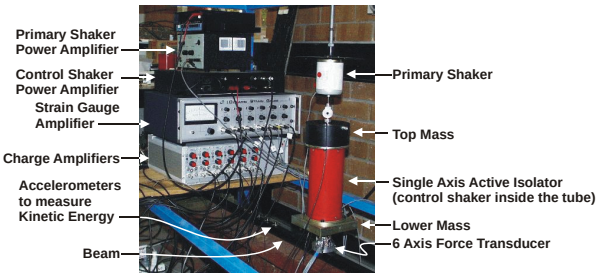

Figure 18: Photo of the experiment setup.

A steel beam, of dimensions 1.55m long by 25mm square, was mounted between two knife edges which provided simply supported end conditions. The 6-axis force transducer, described in Howard (1999) was bolted to the beam, 0.75m

from its end. Attached to the top of the force transducer was the lower mass, which was used to support the end of the vibration isolator. The vibration isolator was a cylindrical polyurethane tube and inside the tube was a Ling Dynamics V203 shaker, which provided a canceling force to counteract the vibrations that passed through the outer tube. On top of the vibration isolator was a solid steel cylindrical mass, which weighed 7.4kg. Five accelerometers were attached to the beam to measure its residual vibration when active control was applied. The five accelerometers were used to measure the approximate KE of the beam and were mounted at 0.30m, 0.35m, 0.40m, 0.45m and 0.50m from its end. Four accelerometers were attached the 6-axis force transducer and these were used to calculate the acceleration of the structure beneath the strain gauges, using the method described in Howard (1999). All the transducers were connected to amplifiers that were connected to the Bruel and Kjær Pulse System, which in turn measured the transfer functions. The primary shaker was connected to the top mass and applied a harmonic force, which swept in frequency between 5Hz to 200Hz.

Method

The vibration isolation performance described here is quantified by the change in approximate kinetic energy (KE) of the beam measured by summing the squared accelerations of 5 accelerometers. This measurement is not affected by phase errors and provides a reasonable approximation of the global KE of the beam. It also provides an independent measure of the isolation performance. Comparisons of the isolation performance using a single sensor, for example the acceleration at the base of the isolator, do not provide a good measure because it is possible to minimise the vibration at the sensor and increase the vibration elsewhere on the supporting structure. The determination of the true value of the KE requires the summation of an infinite number of acceleration measurements over the length of the beam to measure the translational and rotational accelerations. However, the use of five measurement locations provides a reasonable approximation to the exact value.

The physical properties of the simply supported beam and isolator system are shown in Table 1 and are used with the theoretical analysis presented in Howard (1999).

Table 1: Properties of the beam and isolator.

Beam length	1.500m
Beam width	0.025m
Beam thickness	0.025m
Beam density	7800 kg/m^3
Young's modulus	207 GPa
Beam damping	7.48 × 10^{-6} sN/m
Top mass	7.4 kg
Bottom mass	8.2 kg
Moment of inertia	1.6 × 10^{-5} m^4
Isolator location	0.760m
Isolator stiffness *kz*	45870 N/m
Isolator damping *cz*	140 sN/m
Isolator stiffness *kθy*	216 N/rad
Isolator damping *cθy*	140 sN/rad

The method used here to predict the isolation performance of the system requires measured transfer function data. A similar method has been used by Dorling et al. (1987, 1989) where measured acoustic transfer function data were used to predict the sound pressure levels inside an aircraft cabin as a result of active noise control.

Transfer functions were measured between the driving force on the structure and the response at the error sensors. The driving force was measured by placing a force transducer between a shaker and the structure. Response measurements were made at the 6-axis force transducer and the acceleration transducers. Transfer functions were also measured between the primary shaker and the error sensors and between the control shakers and the error sensors.

The error signals from the error sensors can be written in matrix form as (Nelson and Elliot, 1992, Appendix A.5):

$$\mathbf{e} = \mathbf{d} + \mathbf{C}\mathbf{x} \tag{2}$$

where $\mathbf{e}$ is a (n_e x 1) vector of n_e error signals, $\mathbf{x}$ is a (n_c x 1) vector of control signals, $\mathbf{d}$ is a (n_e x 1) vector of the error signals resulting from passive control and $\mathbf{C}$ is a (n_e x n_c) matrix of the transfer functions between the control signals and the error signals when the primary disturbance is turned off. The usual goal of active control systems is to determine the amplitude and phase of the control signals that will cancel the primary disturbance, and is given by re-arrangement of Eq. (2) as:

$$\mathbf{x}_0 = -(\mathbf{C})^{-1}\mathbf{d} \tag{3}$$

Equation (3) can be solved when there are an equal number of control signals and error signals ($n_c = n_e$). If there are more error signals than control signals ($n_e > n_c$) then the problem is said to be over-determined. The matrix $\mathbf{C}$ is not square and cannot be inverted, and generally it is not possible to achieve complete cancelation at all of the error sensors. The problem can be transformed into a least-squares problem such that the cost function J that is minimized is the squared amplitude of the error signals $\mathbf{e}$, which can be written as:

$$J = \mathbf{e}^{\mathrm{H}}\mathbf{e} = \mathbf{x}^{\mathrm{H}}\mathbf{C}^{\mathrm{H}}\mathbf{x} + \mathbf{x}^{\mathrm{H}}\mathbf{C}^{\mathrm{H}}\mathbf{d} + \mathbf{d}^{\mathrm{H}}\mathbf{C}\mathbf{x} + \mathbf{d}^{\mathrm{H}}\mathbf{d} \tag{4}$$

Equation (4) is in the general Hermitian quadratic form, and has a minimum value when the control signals are given by:

$$\mathbf{x}_0 = -(\mathbf{C}^{\mathrm{H}}\mathbf{C})^{-1}(\mathbf{C}^{\mathrm{H}}\mathbf{d}) \tag{5}$$

For the experiments conducted here, which involve the minimisation of the squared value of power transmission, the velocity and forces at the error sensor can be written as:

$$\mathbf{v} = \mathbf{Z}_{vp}\mathbf{f}_p + \mathbf{Z}_{vc}\mathbf{f}_c \tag{6}$$

$$\mathbf{f} = \mathbf{Z}_{fp}\mathbf{f}_p + \mathbf{Z}_{fc}\mathbf{f}_c \tag{7}$$

where $\mathbf{Z}_{ij}$ is a transfer function between velocity or force, i, and primary or control force, j. For example, $\mathbf{Z}_{vc}$ is the transfer function matrix of dimensions (n_e x n_c) between the velocity measured at an error sensor and the driving control force. The transmitted vibrational power is calculated by substituting Eqs. (6) and (7) into Eq. (1), then re-grouping the terms into the format shown in Eq. (4). The details of this lengthy derivation are shown in Howard (1999).

Results

Theoretical and experimental predictions are presented for the approximate KE of a simply supported beam for the cases of passive and active isolation of a vibrating rigid mass that is actively isolated from the beam. It is theoretically possible to stop all of the vibratory energy of the rigid mass from reaching the simply supported beam if the primary force is exactly aligned with the control actuator. In reality, this is difficult to achieve as there is usually a small misalignment between the primary shaker and the centroid of the rigid

mass. For the theoretical results presented in this section, it is assumed that there is 2mm of misalignment, so that the primary load on the top mass is Fz=1N and My=0.002Nm.

The results from Howard et al. (1998) show that active control using signed power transmission (that is, trying to make the power transmission as negative as possible) as a cost function to be minimized will converge to a negative value of power transmission if moments are present and could result in the overall vibration response of the receiving structure being greater than it was with only passive isolation. This is because some of the power transmitted into the beam by moments may be re-transmitted into the mass along the vertical translational axis, resulting in a negative power transmission along the vertical axis. Hence, the experiments conducted here involve the minimisation of the squared value of power transmission.

Figure 19 shows the theoretically predicted KE for passive isolation, when the squared power transmission Pz^2 along the vertical axis is minimized, and when the sum of the squared power transmission $Pz^2 + P\theta y^2$ along the vertical and rotational axes is minimized, for the case when there is a random +/-2 degree phase error. This result shows that phase errors associated with the measurement of power will not greatly affect the minimization of squared power transmission. This prediction was confirmed by experiment as shown in Figure 20. It can be seen that the minimization of squared power transmission along the vertical and rotational axes results in a lower KE of the beam at the rotational resonance of 108Hz. Figure 20 shows that the results for the minimisation of power transmission along the *z*-axis (Pz^2) at 108Hz has higher kinetic energy in the beam than the passive isolation case. This result indicates that vibrational power circulation is occuring, where vibrational power from rotational motion is being redirected into the rigid mass through the vertical axis prior to the application of active control. The application of active control prevents this reverse power transmission through the vertical axis, resulting in higher KE in the beam than if the active control system were turned off.

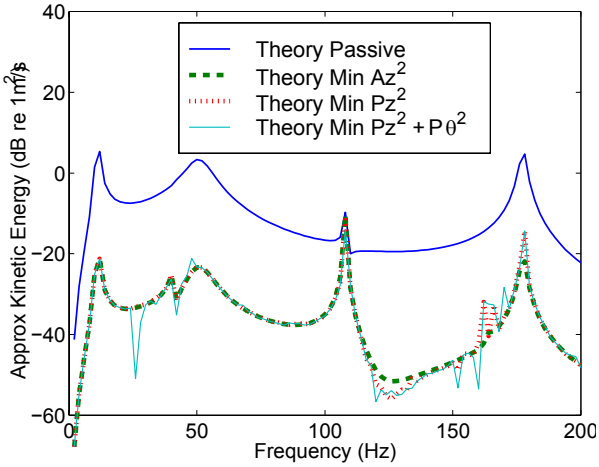

Figure 19: Theoretical prediction of the KE of the beam for passive isolation, minimization of squared acceleration Az^2 along the vertical axis, minimization of squared power transmission Pz^2 along the vertical axis with a random +/-2 degree phase error.

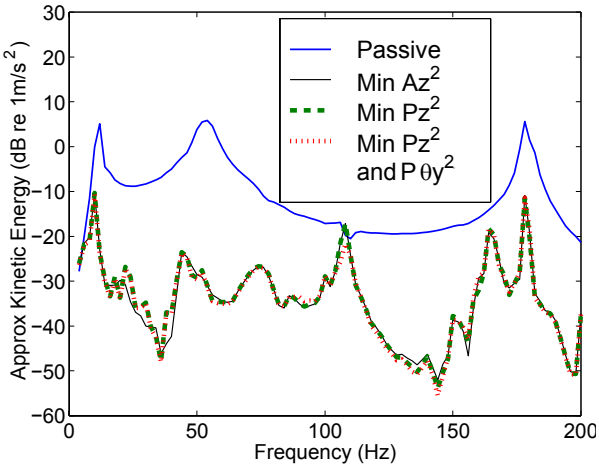

Figure 20: Experimental results of the KE of the beam for passive isolation, minimization of squared acceleration Az^2 along the vertical axis, minimization of squared power transmission Pz^2 along the vertical axis and the minimization of the sum of the squared power transmissions $Pz^2 + P\theta y^2$ along the vertical and rotational axes.

CONCLUSIONS

A transducer was constructed that measures vibratory power transmission along six axes and utilises a force transducer, which can measure forces and moments along several axes, and an accelerometer array mounted to the top and bottom flanges of the force transducer, which measures translational and rotational motion. The force transducer consists of 24 strain gauges mounted on to a cylindrical tube. Sets of four strain gauges were combined into a single full bridge Wheatstone circuit to determine the force or moment along a particular axis. The orientation of the strain gauges was important in minimising cross-axis loads. Experiments were conducted to determine the magnitude and phase accuracy of the force transducer. It was found that the force transducer had good amplitude accuracy; however the phase accuracy of less than 2 degrees was insufficient for highly accurate measurements of power transmission in lightly damped structures with highly reactive vibration fields.

This transducer was used to investigate the effectiveness of actively minimizing the transmission of vibration from a vibrating rigid mass to a simply supported beam. The active isolator was intended to control vibration transmission only along the vertical axis, and the transducer was used as an error sensor allowing minimization of vibration along any translational or rotational axis or combination of axes. The effectiveness of the cost function was evaluated by measuring the vibration levels in the simply supported beam, which acted as the receiving structure. The results from the active vibration isolation experiments demonstrated the existence of the vibrational power circulation phenomena, where vibrational power transmitted by rotational motion can be transformed into reverse power transmission along the vertical translational axis.

REFERENCES

Bardou, O., Gardonio, P., Elliot, S. and Pinnington, R. (1997), 'Active power minimization and power absorption in a plate with force and moment excitation', Journal of Sound and Vibration 208(1), 111–151.

Dorling, C. Eatwell, B., Hutchins, S., Ross, C. and Sutcliff, S. (1987), 'A demonstration of active noise reduction in an aircraft cabin', Journal of Sound and Vibration, 128(2), 358-360.

Dorling, C. Eatwell, B., Hutchins, S., Ross, C. and Sutcliff, S. (1989), 'A demonstration of active noise reduction in an aircraft', Journal of Sound and Vibration, 112(2), 389-395.

Engeler, P. and Giorgetta, M. (1995), 'Multi-component force and moment measuring arrangement', United Stated Patent 5,402,684.

Gialamas, T., Tsahalis, D., Bregant, L., Otte, D. and van der Auweraer, H. (1996), Rotational degrees of freedom: an investigation of their influence on the prediction of the dynamic behaviour of a coupled structure, in F. Hill and R. Lawrence, eds, 'Proceedings of InterNoise '96', Vol. 3, Institute of Acoustics, 5 Holywell Hill, St Albans, UK, Liverpool, UK, pp. 1395–1399.

Gibbs, B. and Yap, S. (1998), The contribution of forces and moments to the structure-borne sound power from machines rigidly attached to supporting floors, in 'Proceedings of InterNoise '98', INCE, Christchurch, New Zealand.

Hoffmann, K. (1976), Measuring elementary load cases with strain gauges (vd73002e), Hottinger Baldwin Messtechnik GMBH, West Germany.

Horner, J. L. and White, R. G. (1990), Techniques for measuring vibrational power transmission in a beam like structure carrying two types of wave, in 'Structural Intensity and Vibrational Energy Flow 3rd International Congress on Intensity Techniques', CETIM, Senlis, France, pp. 273–280.

Howard, C. Q. (1999), Active isolation of machinery vibration from flexible structures, PhD thesis, University of Adelaide, Australia.

Howard, C. Q. and Hansen, C. H. (1999), 'Finite element analysis of active vibration isolation using vibrational power as a cost function', International Journal of Acoustics and Vibration 4(1), 23–36.

Ji, L., Mace, B. and Pinnington, R. (2003), 'A power mode approach to estimating vibrational power transmitted by multiple moments', Journal of Sound and Vibration 265, 387–399.

Kaneko, M. (1996), 'Twin head six-axis force sensor', IEEE Transactions on Robotics and Automation 12(1), 146–154.

Koh, Y. K. and White, R. G. (1997a), 'Analysis and control of vibrational power transmission to machinery supporting structures subjected to a multi-excitation system, Part I: driving point mobility matrix of beams and rectangular plates', Journal of Sound and Vibration 196(4), 469–493.

Koh, Y. K. and White, R. G. (1997b), 'Analysis and control of vibrational power transmission to machinery supporting structures subjected to a multi-excitation system, Part II: vibrational power analysis and control schemes', Journal of Sound and Vibration 196(4), 495–508.

Koh, Y. K. and White, R. G. (1997c), 'Analysis and control of vibrational power transmission to machinery supporting structures subjected to a multi-excitation system, Part III: vibrational power cancellation and control experiments', Journal of Sound and Vibration 196(4), 509–522.

Mondot, J. and Moorhouse, A. (1996), The characterisation of structure borne sound sources, in 'Proceedings of InterNoise '96', Vol. 3, INCE, Liverpool, UK, pp. 1439–1442.

Moorhouse, A. (2002), 'A dimensionless mobility formulation for evaluation of force and moment excitation', Journal of the Acoustical Society of America 112(3), 972–980.

Nelson, P.A, and Elliot, S.J. (1992), Active control of sound, Academic Press Ltd, San Diego.

Petersson, B. (1993a), 'Structural acoustic power transmission by point moment and force excitation, Part I: Beamand framelike structures', Journal of Sound and Vibration 160(1), 43–66.

Petersson, B. (1993b), 'Structural acoustic power transmission by point moment and force excitation, Part II: Platelike structures', Journal of Sound and Vibration 160(1), 67–91.

Petersson, B. A. T. and Gibbs, B. M. (1990), The influence of source location with respect to vibrational energy transmission, in '3rd International Congress on Intensity Techniques', CETIM, Senlis, France, pp. 449–456.

Quinn, T. P. and Mote Jr., C. D. (1990), 'Optimal design of an uncoupled six degree of freedom dynamometer', Experimental Mechanics 30(1), 40–48.

Sanderson, M. (1996), 'Vibration isolation: moments and rotations included', Journal of Sound and Vibration 198, 171–191.

Sanderson, M. A., Fredo, C. R., Ivarsson, L. I. and Gillenang, M. (1995), Transfer path analysis including internal force and moment strength estimations at vibration isolators, in 'Proceedings of InterNoise '95', INCE, Newport Beach, CA, USA, pp. 1407–1410.

Shepard Jr., W. (2002), 'Comparison of moments and couplegenerating forces near discontinuities in structuralacoustic systems', Journal of the Acoustical Society of America 111(4), 1718–1725.

Skudrzyk, E. (1968), Simple and complex vibratory systems, The Pennsylvania State University Press, USA.

Yap, S. and Gibbs, B. (1999a), 'Structure-borne sound transmission from machines in buildings, part 1: indirect measurement of force at the machinereceiver interface of a single and multipoint connected system by a reciprocal method', Journal of Sound and Vibration 222(1), 85–98.

Yap, S. and Gibbs, B. (1999b), 'Structure-borne sound transmission from machines in buildings, part 2: indirect measurement of force and moment at the machinereceiver interface of a single point connected system by a reciprocal method', Journal of Sound and Vibration 222(1), 99–113.